JOURNAL OF THERMOPHYSICS AND HEAT TRANSFER
Vol. 16, No. 1, January–March 2002

Unsteady, Conjugated Duct Heat Transfer Solution with Wall Heating

James Sucec*
University of Maine, Orono, Maine 04469-5711
and
Hong-Zhao Weng†
General Electric Aero Energy Products, Houston, Texas 77015

An analytical model for time-varying surface heat flux, consisting of two integrals, is used to solve for the wall temperature and fluid bulk mean temperature distributions as a function of axial position and time. This is done for a parallel plate duct with generation occurring in the duct walls. A solution is found using the Laplace transform for the case of generation rate varying linearly with axial position, a situation for which the flux model is exact at small time. A solution, using the flux model, is also found for a wall generation rate that is linear axially and exponential in time. Results from the two integral flux model used are compared to results with a finite difference solution of the governing partial differential equation. Comparisons are also made to a much simpler quasi-steady analysis.

Nomenclature

B	=	ratio of thermal capacity of the wall to the fluid, $\rho_w c_{pw} b/\rho_f c_{pf} R$
b	=	duct wall thickness
c_{pf}, c_{pw}	=	specific heat capacity of fluid and of wall
f	=	q'''/q_g
h	=	coefficient of heat transfer at inside duct wall
k_f	=	thermal conductivity of fluid
Nu	=	Nusselt number, hR/k_f
R	=	half height of duct
T, T_i, T_B, T_W	=	local, initial, bulk mean, and wall temperatures
u_m, $u_{\max}$	=	mass averaged and maximum velocity
x	=	space coordinate along the wall
y	=	space coordinate perpendicular to duct wall
α_f	=	thermal diffusivity of fluid
ΔF, ΔX	=	finite difference increments in F and X
ρ_f, ρ_w	=	mass density of fluid and of wall
ϕ	=	nondimensional local temperature, $k_f(T - T_i)/q_g bR$

Subscripts

B	=	bulk mean fluid value
qs	=	quasi-steady value
w	=	duct wall value

Introduction

FOR flow within a duct under unsteady-state conditions, the heat transfer problem for the engineer is often the prediction of the wall surface heat flux and the fluid bulk mean temperature as a function of position and time. These unsteady-state conditions occur during start-up and shut-down operations, as well as changes in the steady-state operation levels of coolant passages in various types of equipment such as heat exchangers and nuclear power reactors.

Realistically, many of those transient problems are so called conjugate problems, where one knows neither the wall surface temperature distribution nor the wall heat flux distribution. Rather, both of these must be found by solution of the problem using the fact that both the unknown flux and wall temperature must be continuous at the fluid solid wall interface.

The simplest approach to a transient conjugated problem is the quasi-steady approach, which uses a constant value of the surface coefficient of heat transfer h. This approach has often been taken in unsteady heat exchanger problems such as by Spiga and Spiga.[1] However, quasi-steady results are often limited by the ratio of wall thermal capacity to that of the fluid and by the rapidity of the transient.

Solutions, which do not employ the quasi-steady approximation to laminar transient, conjugated heat transfer within a pipe have been found by Olek,[2] using an eigenfunction expansion, and by Al-Nimr and Hader[3] and by Lin and Kuo,[4] using finite difference methods. The solutions were for boundary conditions of prescribed temperature or heat flux at the outside wall surface. Solutions to similar duct flow problems, but with a periodically varying inlet temperature of the fluid, are given for slug flow by Travelho and Santos[5] using Laplace transforms.

The present work predicts the surface heat flux and duct wall and bulk mean fluid temperatures as a function of axial distance and time. It uses the flux model, developed in Ref. 6, to solve conjugated problems that have generation within the duct wall as occurs in nuclear fuel elements and electric resistive heating. The flux model in Ref. 6 was applied to cases of steady, specified wall temperature. Considered here is the initial, and often the most rapid, part of the transient, the time regime where $t < x/u_{\max}$. These are times less than the fastest moving fluid would take to travel from the duct entrance, at the start of the transient, to the axial x position of interest. We refer to this as the first time domain. An approximate, two-integral heat flux model presented by Sucec and Radley[6] will be used. The flux model in Ref. 6 was developed for a wall temperature that is a given, arbitrary function of axial position x and time t. In the present work it is applied to a conjugate problem by using it in the energy balance on the duct wall. The resulting integro–differential equation will be solved by Laplace transforms for a generation rate linear in x and by numerical methods for a more complicated time-dependent generation rate. Comparisons will be made to the simpler quasi-steady solutions and also to finite difference solutions to the governing partial differential equations for the fluid and the wall. The solutions of this work can be used as baseline results for validation of finite difference or finite element computer codes in this general type of problem.

Received 2 February 2001; revision received 5 July 2001; accepted for publication 9 July 2001.

*Professor, Mechanical Engineering Department, 5711 Boardman Hall.
†Mechanical Engineer, Engineering Department, 16415 Jacintoport Boulevard.

Analysis

We consider steady, laminar fluid flow, with a fully developed velocity field in the thermal entrance region of a parallel plate duct. The duct walls are spaced a distance $2R$ apart with a wall thickness b. Initially, both the walls and the moving fluid are at a known, constant, uniform temperature T_i. Suddenly, at time $t = 0$, a generation rate per unit volume, q''', is turned on in the duct wall and may, in general, be dependent on axial position x and time t. We wish to predict the duct wall temperature, surface heat flux, and fluid bulk mean temperature as a function of x and t. Axial conduction in both the wall and the fluid are neglected as is viscous dissipation. The transverse Biot number will be small enough to allow the temperature profile to be lumped across the duct wall thickness b. We seek a solution in the first time domain, $t < x/u_{\max}$. After writing $q''' = q_g f(x, t)$, where q_g has the same units as q''', namely, watts per cubic meter, an energy balance on an element of duct wall b thick by dx long, when the outside of the wall is insulated, yields

$$\rho_w c_{pw} b \frac{\partial T_w}{\partial t} + q_w(x, t) = q_g f(x, t) b \tag{1}$$

where $q_w(x, t)$ is the local surface heat flux (watts per square meter) from the wall to the fluid in the duct. Equation (1) is where the conjugation conditions, continuity of temperature, and heat flux at the fluid–wall interface, are incorporated into the analysis.

The nondimensional quantities to be used are defined as $F = \alpha_f t/R^2$, $Y = y/R$, $X = \alpha_f x/R^2 u_m$, $Q = q_w/q_g b$, $\phi_w = k_f (T_w - T_i)/q_g b R$, $\phi_B = k_f (T_b - T_i)/q_g b R$, and $B = \rho_w c_{pw} b/\rho_f c_{pf} R$.

After transforming to a new X-like independent variable, $\tau = F - X$, as in Ref. 6, Eq. (1) can be written as follows:

$$\left[\frac{\partial \phi_w}{\partial F} + \frac{\partial \phi_w}{\partial \tau}\right] + \frac{Q(F, \tau)}{B} = \frac{f(F, \tau)}{B} \tag{2}$$

This is subject to the initial condition, namely,

$$F = 0, \qquad \tau < 0, \qquad \phi_w = 0 \tag{3}$$

Note that because we are dealing with the first time domain, $F < 2X/3$, no boundary condition is needed on the X-like independent variable τ.

The two-integral approximate model to be used for the nondimensional flux, $Q(F, \tau)$ was developed by Sucec and Radley[6] and is exact if ϕ_w varies linearly with X, but is approximate otherwise. It is given as follows:

$$Q = \frac{1}{\sqrt{\pi}} \left\{ \int_0^F (F - \sigma)^{-\frac{1}{2}} \frac{\partial \phi_w}{\partial \sigma} \, d\sigma - \int_0^F \left[\frac{a_1 \sqrt{F - \sigma}}{2\sqrt{\pi}} + \frac{a_0}{4} - \frac{(F - \sigma)^{-\frac{1}{2}}}{2\sqrt{\pi}} \right] \frac{\partial \phi_w}{\partial \tau} \, d\sigma \right\} \tag{4}$$

where a_0 and a_1 are coefficients in the velocity profile, which for a laminar, fully developed duct flow can be written, with $a_0 = 3$ and $a_1 = -\frac{3}{2}$, as

$$u(Y)/u_m = a_0 Y + a_1 Y^2 \tag{5}$$

As can be shown, the first integral in the expression for $Q(F, \tau)$, in Eq. (4) is the exact solution for a slug velocity profile, whereas the second integral, in this flux model, accounts for the actual nonslug velocity distribution. Sucec and Radley[6] showed that Eq. (4) is the exact expression for Q when ϕ_w varies linearly with X. Even for higher harmonics in ϕ_w, such as ϕ_w proportional to X^6, it was found that there was negligible difference between Eq. (4) and the exact solution. Equation (4) was developed for a thermal boundary layer. Thus, strictly speaking, when it is exact for Q, it will be so for small times F, where the thermal boundary-layer thickness is not a large fraction of R. In fact though, as will be seen later, the approximate expression for Q often does very well up to the end of the transient thermal entrance region.

We first look at the case where the generation rate per unit volume, q''', is a linear function of X, $q''' = q_g(1 + CX)$ or $q''' = q_g[1 + C(F - \tau)]$, in F, τ variables. Using this in Eq. (2), as well as the flux model, Eq. (4), gives the following integro–differential equation to be solved for $\phi_w(F, \tau)$:

$$\frac{\partial \phi_w}{\partial F} + \frac{\partial \phi_w}{\partial \tau} + \frac{1}{B\sqrt{\pi}} \int_0^F (F - \sigma)^{-\frac{1}{2}} \frac{\partial \phi_w}{\partial \sigma} \, d\sigma - \frac{1}{B\sqrt{\pi}} \int_0^F \left[\frac{a_1 \sqrt{F - \sigma}}{2} + \frac{a_0 \sqrt{\pi}}{4} - \frac{(F - \sigma)^{-\frac{1}{2}}}{2} \right] \frac{\partial \phi_w}{\partial \tau} \, d\sigma = \frac{1 + C(F - \tau)}{B} \tag{6}$$

Analytical Solution

Noting that the two integrals in Eq. (6) have the form of convolution integrals, we take the Laplace transform with respect to F of Eq. (6) and use the initial condition that at $F = 0$, all τ, $\phi_w = 0$. The inverse transform is then found. When this is done, the solution for the nondimensional wall axial temperature distribution, after changing back to the original variables, F and X, is given by the next equation for the case where $q''' = q_g(1 + CX)$:

$$\phi_w = [C_0 + BC(F - X)]\left(1 - 2\sqrt{F}\Big/B\sqrt{\pi}\right) + C_2 F + \left(C_3\Big/\sqrt{\pi}\right)F^{\frac{3}{2}} + C_4 F^2 + \left(C_5\Big/\sqrt{\pi}\right)F^{\frac{5}{2}} + [C_7 F - C_0 - BC(F - X)] \exp(F/B^2) \operatorname{erfc}\left(\sqrt{F}\Big/B\right) \tag{7}$$

The coefficients, C_0, C_2, C_3, etc., are algebraic functions of B, C, a_0, and a_1, and are given in the Appendix. Examination of Eq. (7) shows that the wall temperature varies linearly with X at any time F. Because the two integral flux model, Eq. (4), being used is exact for linear in X wall temperature at small enough F, we are also getting the exact solution to this case where the generation rate per unit volume is $q''' = q_g(1 + CX)$.

Surface Heat Flux

To find the nondimensional surface heat flux $Q(X, F)$, we return to the basic energy balance [Eq. (2)] and solve for Q. Hence,

$$Q = f(F, \tau) - B\left(\frac{\partial \phi_w}{\partial F} + \frac{\partial \phi_w}{\partial \tau}\right) \tag{8}$$

For the generation rate linear in X, we have that $f(F, \tau) = 1 + C(F - \tau)$. Using this and differentiating Eq. (7) to evaluate the remaining two terms on the right side of Eq. (8) leads to the following expression for $Q(F, X)$:

$$Q = 1 - A_1 + CX + 2A_1\sqrt{F}\Big/B\sqrt{\pi} - A_2 F + A_3 F^{\frac{3}{2}}\Big/\sqrt{\pi} + [A_1 - 1 + C_7 F/B + C(F - X)] \exp(F/B^2) \operatorname{erfc}\left(F\Big/\sqrt{B}\right) \tag{9}$$

A_1, A_2, A_3, and C_7 are given in the Appendix.

Bulk Mean Temperature

The definition of fluid bulk mean temperature gives

$$\phi_B = \int_0^\infty \frac{u(y)}{u_m} \phi(F, \tau, Y) \, dY \tag{10}$$

The upper limit has been used as ∞ because we are in the thermal entrance region of the flow. The operations needed in Eq. (10) have been done for general, arbitrary $\phi_w(F, \tau)$ by Sucec and Radley[6] with the following result:

$$\phi_B = \int_0^F \left[a_0 + \frac{4a_1\sqrt{F-\sigma}}{\sqrt{\pi}} \right] \phi_w(\sigma,\tau)\,d\sigma + \int_0^F \left[-a_0(F-\sigma) + \left(\frac{8}{3}a_0^2 - 4a_1 \right) \frac{(F-\sigma)^{\frac{3}{2}}}{\sqrt{\pi}} + \frac{27}{4}a_0 a_1 (F-\sigma)^2 + \frac{44a_1^2(F-\sigma)^{\frac{5}{2}}}{3\sqrt{\pi}} \right] \frac{\partial \phi_w}{\partial \tau}\,d\sigma \tag{11}$$

Equation (11), like the earlier used two-integral flux model, Eq. (4), is approximate. However, because the present case of generation led to a ϕ_w varying linearly with X, a situation where both Eqs. (4) and (11) are exact at small F, we are getting the exact solution here.

For this case, ϕ_w and $\partial\phi_w/\partial\tau$, with $\tau = F - X$, are found from Eq. (7). Doing this leads to a rather lengthy expression for ϕ_B, one that consists of the addition of 18 separate groups, where each group contains anywhere from 5 to 10 separate functions of nondimensional time F and position X. Space prohibits listing these here, but they are available in Ref. 7.

Next, consider the more complicated generation that is dependent linearly on X and exponentially on time F, namely,

$$q''' = q_g(1 + CX)e^{gF} \tag{12}$$

Equation (12) was used to apply the flux model [Eq. (4)] in some fast transients by using different values for the constant g. In addition, Eq. (12) is of a form that simulates a start up or change in power level of a nuclear fuel plate. Predictions for these two different generation rates will be presented in the "Results and Discussion" section. It was decided to forgo the analytical solution to Eq. (6) when q''' is given by Eq. (12) and, instead, to solve the integro–differential equation numerically. The numerical algorithm used was developed in Ref. 8. In the numerical solution of Eq. (6) employing the flux model [Eq. (4)], the equation for the wall temperature was solved using successively finer lattice spacings, ΔF and $\Delta\tau$. This was continued until the solutions were essentially independent of these lattice spacings. For instance, in a case where $B = 0.10$, the lattice spacings were continually cut in half until the changes in ϕ_w, ϕ_B, and Q were less than 0.2% leading to spacing values of $\Delta\tau = 0.002$ and $\Delta F = 0.0005$.

Finite Difference Solution Without Using the Flux Model

To test the two-integral flux model of Eq. (4), it was decided to get some solutions for comparison by solving the exact partial differential equation by finite differences. For laminar constant property, fully developed flow in a parallel plate duct, the governing partial differential equation for nondimensional temperature, $\phi(X, F, Y)$ can be written as follows along with the initial and boundary conditions:

$$\frac{\partial\phi}{\partial F} + 3\left[Y - \frac{Y^2}{2} \right] \frac{\partial\phi}{\partial X} = \frac{\partial^2\phi}{\partial Y^2} \tag{13}$$

$$F = 0, \quad X > 0, \quad 0 \le Y \le 1, \quad \phi = 0$$

$$X = 0, \quad F > 0, \quad 0 < Y \le 1, \quad \phi = 0$$

$$Y = 1, \quad F > 0, \quad X > 0, \quad \frac{\partial\phi}{\partial Y} = 0$$

$$Y = 0, \quad X > 0$$

$$F > 0 - \left(\frac{\partial\phi}{\partial Y} \right) + B\frac{\partial\phi}{\partial F} = \frac{q'''}{q_g} = f(X, F) \tag{14}$$

The last condition in Eq. (14), at $Y = 0$, is found by an energy balance on the wall of thickness b together with the conjugation conditions of continuity of temperature and heat flux at $Y = 0$, the interface between the solid and the fluid.

The implicit finite difference equations are given by Sucec,[9] where compatibility, truncation error, and the unconditional stability of the equations is discussed. The finite difference lattice spacings ΔX, ΔY, and ΔF were refined to the point where the finite difference solution was essentially independent of the increment sizes being used. For a representative case where $q''' = q_g(1 + CX)\,e^{gF}$, $C = 1$, $g = 10$, and $B = 10$, it was determined that the use of 97 nodes across the duct, $\Delta X = 0.025$ and $\Delta F = 0.00015625$ gave a change in ϕ_w and ϕ_B less than 0.25% relative to spacings twice as large.

Quasi-Steady Solution

This is a common, approximate approach to transient convection problems in which the local surface heat flux $q_{w\text{qs}}$ is given by Newton's cooling law using a constant steady-state surface coefficient h during the transient,

$$q_{w\text{qs}} = h(T_w - T_B) \tag{15}$$

In this approach, one uses Eq. (15) and makes an energy balance on a length dx of the duct wall and also on the same length of fluid. Doing this gives the following two partial differential equations in terms of the nondimensional quantities being used in the present work. The Nusselt number is $Nu = hR/k_f$:

$$\frac{\partial\phi_B}{\partial F} + \frac{\partial\phi_B}{\partial X} = Nu(\phi_w - \phi_B) \tag{16}$$

$$B\frac{\partial\phi_w}{\partial F} + Nu(\phi_w - \phi_B) = f(X, F) \tag{17}$$

Their boundary and initial conditions are as follows:

$$F = 0, \quad X > 0, \quad \phi_B = \phi_w = 0$$

$$X = 0, \quad F > 0, \quad \phi_B = 0 \tag{18}$$

Exponential in F, Linear in X Generation

These equations were solved by taking the Laplace transform of both with respect to F and eliminating $\bar{\phi}_w$ between the two equations. This gave an equation for $\bar{\phi}_B$ that was solved by a second Laplace transform with respect to X. After inverting, this results in the following:

$$\phi_{B\text{qs}} = J_1 e^{gF} + (J_2 + J_4 F)e^{-wF} + J_3 + J_5 F \tag{19}$$

$$w = Nu + Nu/B \tag{20}$$

J_1, J_2, and J_3 depend on position X, w, g, Nu, and B, whereas J_4 and J_5 have no X dependence. These expressions are given in the Appendix.

Now that $\phi_{B\text{qs}}$ is known as a function of X and F, it was used in Eq. (17), and that differential equation was solved by standard mathematical techniques. This gives the quasi-steady wall temperature distribution as

$$\phi_{w\text{qs}} = E_0 + E_1 F + E_2 e^{-gF} + (E_3 + E_4 F)e^{-wF} - (E_0 + E_2 + E_3)e^{-NuF/B} \tag{21}$$

As was the earlier case for J_1, J_2, and J_3, E_0, E_2, and E_3 depend on position X, as well as w, g, Nu, and B, whereas E_1 and E_4 have no X dependence. E_0, E_1, E_2, etc., are given in the Appendix in terms of J_1, J_2, and so on.

We are reminded that these solutions for $\phi_{B\text{qs}}$ and $\phi_{w\text{qs}}$ have been found and are limited to the first time domain, namely, for $F < 2X/3$. However, when getting these quasi-steady solutions, the mathematics formally requires only that $F < X$.

Generation Linear in X

For this case, the quasi-steady solutions are

$$\phi_{B\text{qs}} = K_0 + K_1 F + K_2 F^2 + (K_3 + K_4 F)e^{-wF} \tag{22}$$

$$\phi_{w\text{qs}} = G_0 + G_1 F + G_2 F^2 + (G_3 + G_4 F)e^{-wF} - (G_0 + G_3)e^{-NuF/B} \tag{23}$$

Some of the various K and G in Eqs. (22) and (23) depend on position X. These coefficients are given in the Appendix. To calculate

values from the quasi-steady relations, the value of the constant, steady-state Nusselt number Nu is needed. The constant flux Nusselt number Nu was used, namely, $Nu = 2.055$. For the types of problems being considered here, the quasi-steady solution entails a fair amount of effort and yet, often, this quasi-steady solution will not be accurate enough. This will be seen in some of the comparisons that are made in the following section.

Results and Discussion

Figures 1–6 show some representative results using the two-integral flux model of this work [Eq. (4)] the quasi-steady solution functions, and finite difference solutions, all in the first time domain, $F < 2X/3$. For a wall generation rate per unit volume varying linearly with X, predictions of the nondimensional wall temperature ϕ_w, fluid bulk mean temperature ϕ_B, and surface flux Q are shown in Fig. 1, for these solutions vs nondimensional time F. In addition, some representative predictions of the finite difference solution are given. As explained earlier, for this linear in X generation rate, the approximate flux model being used is exact at small F. Hence, it is seen that the analytical results using this model, the solid curves, are coincident (within plotting ability) with the finite difference results, the circles with dot. There is a slight difference between the Q values predicted at $F = 0.35$, which is due to the flow being just beyond the thermal entrance region because the finite difference results give a centerline temperature just above zero at $F = 0.35$. Even so, the agreement is virtually perfect for ϕ_w and ϕ_B at $F = 0.35$. The quasi-steady solution is shown as dashed curves. The quasi-steady flux is low, as one would expect, because of the use of the steady-state Nusselt number, which is always lower than the true, transient Nusselt number. This leads to the quasi-steady wall temperature being too high. The value of B, the ratio of the thermal storage capacity of the wall to that of the fluid, is $B = 1.0$ in Fig. 1, and it is seen that the quasi-steady results are not good enough except for, possibly, the bulk mean temperature ϕ_B.

Figure 2 shows the influence of the thermal capacity storage parameter B on the predicted wall temperature at position $X = 1.0$ for the generation rate linear in X. The solid curves are the solution using the flux model and, for this generation rate, also are the exact solution at small F. Because the finite difference results virtually coincide with these solid curves, they are not shown in Fig. 2. As seen from Fig. 2, as B decreases from 10 down to 0.10, the wall temperature ϕ_w, increases at any given time F. This makes physical sense because as B decreases, so does the thermal storage capacity of the wall material relative to the fluid. Hence, for a given amount of energy generated, or liberated, within the wall, higher wall temperatures occur as B is lowered. The quasi-steady solution, the dashed

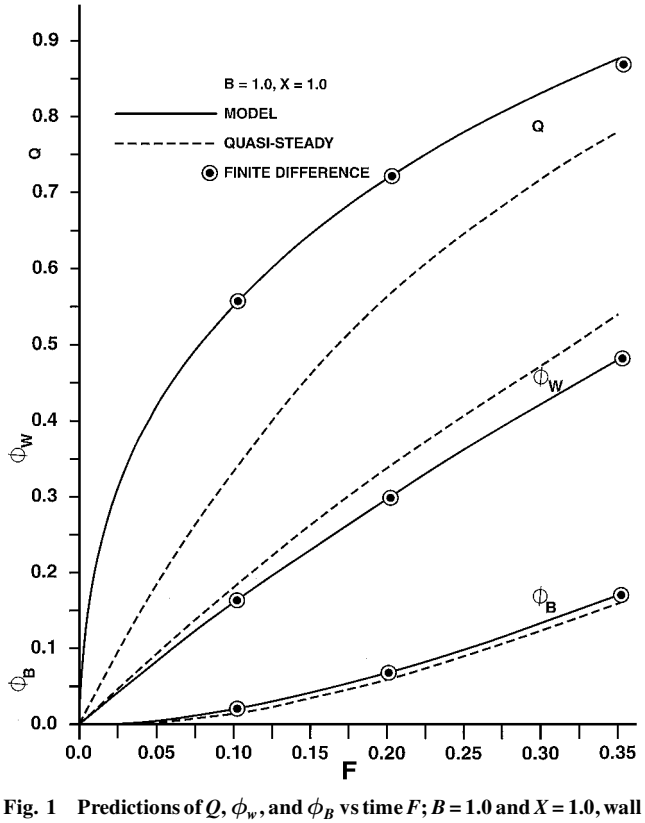

Fig. 1 Predictions of Q, ϕ_w, and ϕ_B vs time F; $B = 1.0$ and $X = 1.0$, wall generation linear in X.

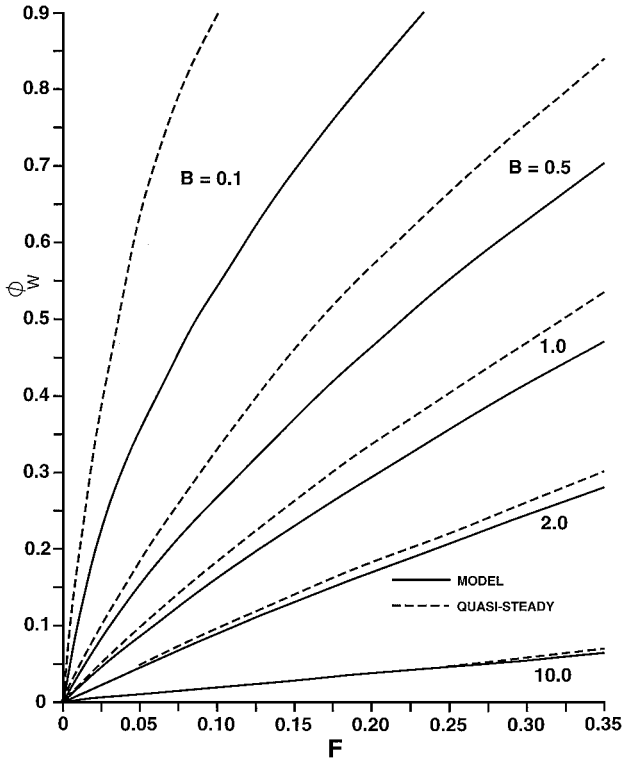

Fig. 2 Predicted wall temperature vs time showing influence of B; $X = 1.0$, wall generation linear in X.

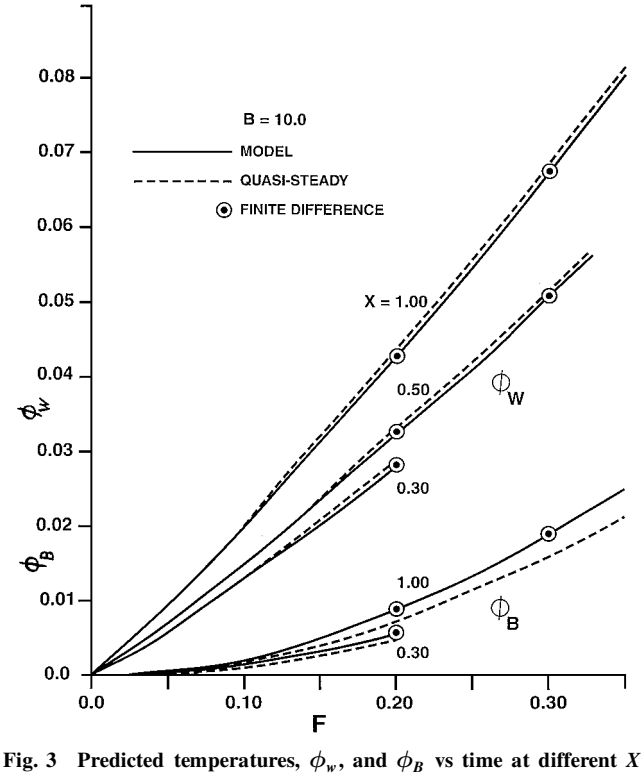

Fig. 3 Predicted temperatures, ϕ_w, and ϕ_B vs time at different X locations; wall generation linear in X and exponential in time F: $g = 1.0$.

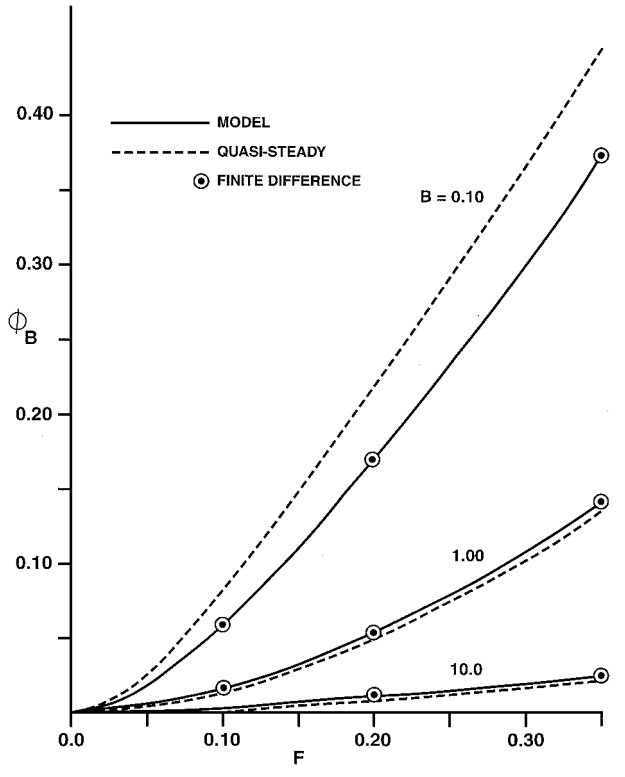

Fig. 4 Predicted fluid bulk mean temperature vs time showing influence of B; wall generation linear in X and exponential in time: $g = 1.0$, $X = 0.50$ for $B = 0.10$ and 1.0, $X = 1.00$ for $B = 10.0$.

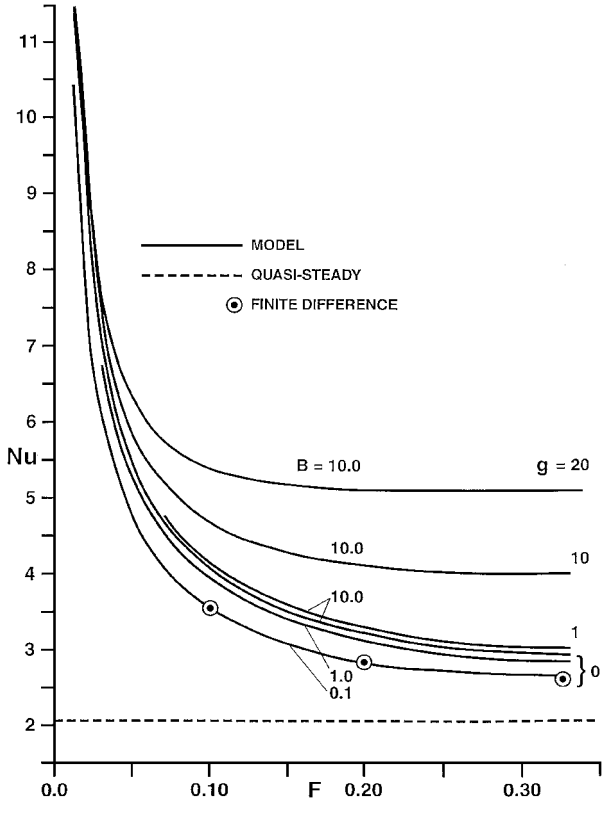

Fig. 6 Transient Nusselt number predictions showing influence of B and g; wall generation linear in X and exponential in F.

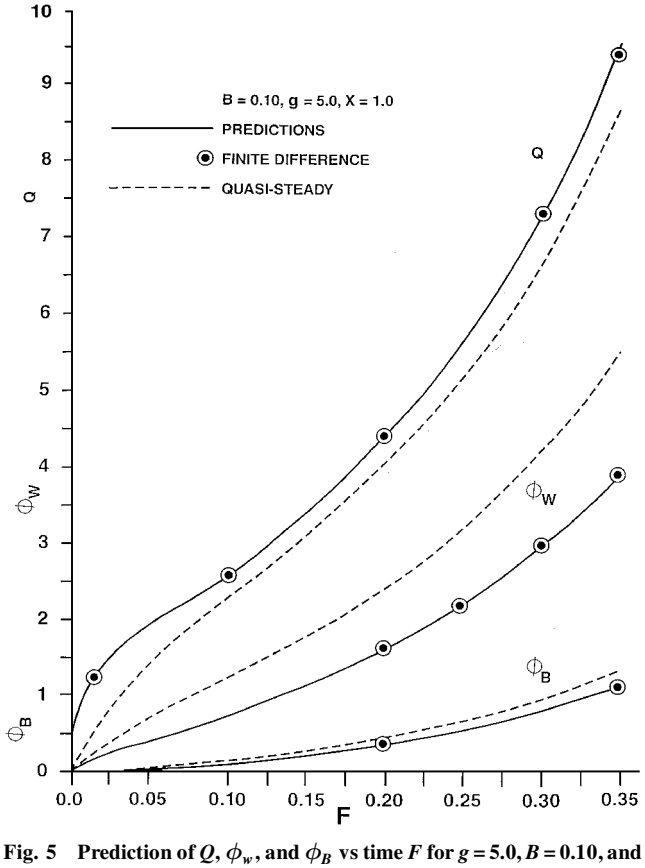

Fig. 5 Prediction of Q, ϕ_w, and ϕ_B vs time F for $g = 5.0$, $B = 0.10$, and $X = 1.0$; wall generation linear in X and exponential in F.

curves, are seen to be greatly in error for all values of B shown except for $B = 10.0$. At $B = 10.0$, the large thermal capacity of the wall material holds so much of the generated energy that the surface flux is relatively small. This makes the transient so slow that the fluid really is passing close enough to a sequence of steady states to allow the quasi-steady approximation to be a good one, at least as far as the wall temperature ϕ_w is concerned. This conclusion concerning the validity of the quasi-steady result for ϕ_w, when $B \geq 10$, is also supported by previous work,[10] in a different type of transient, where the parameter used was $\hat{a}$, which is one over B. The particular values of B for which results are calculated were dictated by the practical range of combinations of wall material and thickness and type of fluid. This is discussed in Ref. 9, and more evidence for the range of B is given by Romie[11] and Karvinen.[12]

Figures 3–6 are all for a generation rate per unit volume linear in X and exponential in time, $q''' = q_g(1 + CX)e^{gF}$. For this generation rate, an analytical solution was not pursued, and instead the numerical solution with the approximate flux model was employed. In the development of this numerical solution, it was tested first by application to the linear in X, constant in time, generation rate for which an exact solution, at small F, and finite difference solution had already been found. When this numerical solution was compared to the results in Figs. 1 and 2, it was found to be virtually identical and gave confidence in its integrity, and so it was then applied to the more complex generation rate $q_g(1 + CX)e^{gF}$.

Figure 3 shows computed results for ϕ_w and ϕ_B vs time F, at different axial locations X, when $B = 10$ and $g = 1.0$. It is seen that the finite difference results lie virtually on top of the solid curves representing the numerical solution with the flux model. The maximum difference between them is less than 0.3%; hence, only a few representative points are shown for the finite difference solution. The reason for the curves at $X = 0.30$ and 0.50 ending at $F = 0.20$ and 0.333 is due to that being the end of the first time domain because F must be less than or equal to $2X/3$. Simply out of curiosity, the analytical solution for ϕ_w [Eq. (7)] was calculated beyond the end of time domain I, and also beyond the thermal entrance region, and the results were compared to the finite difference solution, which

does not have these limitations. Surprisingly, it was found that, for generation equal to $q_g(1+CX)$ and $B=1.00$, the analytical results did surprisingly well. For example, at $X=0.5$, where time domain I ends at $F=0.333$, ϕ_w was predicted to within 1.0% of the correct value all of the way to $F=0.90$ using the first time domain solution. It seems as if the present first time domain solution might have some limited validity well beyond that time. Now, looking at the quasi-steady results, the dashed curves in Fig. 3, we see that for $B=10.0$, the agreement of the quasi steady ϕ_w is good, as we expected from the discussion of quasi-steady results in Fig. 2, relative to the value of B. In fact, the error in quasi steady ϕ_w is less than 1.5% at $B=10$. However, the quasi steady ϕ_B is not that good, with an error of about 21% at $F=0.10$ reducing to around 14% at $F=0.35$. Hence, if accurate prediction of ϕ_B is important, as it is in heat exchangers and many other coolant passages, even a value of $B=10$ may not be large enough to rely on the quasi-steady results for ϕ_B in the analysis of the coolant flow.

Figure 4 shows predictions of the variation of bulk mean fluid temperature vs time, at fixed X, for different ratios B of the thermal storage capacity of solid and fluid. This is for the same generation rate, $q_g(1+CX)e^{gF}$, with $C=1$ and $g=1$, as used in Fig. 3. As is seen for a fixed time F and position X, the bulk mean temperature ϕ_B increases with decreasing values of B. This is due to less of the generated energy being able to be stored in the relatively low-thermal capacity solid when B gets smaller, from 10 to 0.1, and therefore, by conservation of energy, this energy goes to the fluid, increasing its bulk temperature ϕ_B. The predictions using the flux model, the solid lines, are again so close to the finite difference results that only a few representative finite difference calculations are shown in Fig. 4. The quasi-steady results shown indicate its significant error, even at $B=10$, as was discussed earlier in connection with Fig. 3.

Even though the flux model used is, except for small F, approximate, it gives very good predictions for the cases considered. The maximum deviation from the finite difference solution of the governing partial differential equation [Eq. (13)] is 0.4% for ϕ_w, 1.1% for ϕ_B, and 1.3% for Q. All of these occur at the largest time used, $F=0.35$, and the maximum X used, $X=1.0$. At smaller values of F, the agreement is generally within a few tenths of a percent.

The predicted heat flux and wall and bulk mean temperatures, Q, ϕ_w, and ϕ_B, are plotted vs time F, in Fig. 5, for $B=0.10$ and for a more rapid transient than those dealt with earlier. Here the multiplier g in the exponential with time portion of the generation rate has been chosen as $g=5$. In spite of the rapid rate at which ϕ_w and ϕ_B are changing with time F, the solution using the flux model is very close to the finite difference results. Not very surprisingly, in view of the small value of B and the rapidity of the transient, there is a lot of error exhibited by the quasi-steady results, the dashed curves, ranging from 66 to 40% for ϕ_w and from 36 to 22% for ϕ_B.

Transient Nusselt numbers, hR/k_f, are plotted vs nondimensional time F, in Fig. 6. The lowest three curves are for the generation rate proportional to $q_g(1+CX)$ and for three different values of the thermal storage capacity ratio B, namely 0.1, 1.0, and 10.0. All results shown are for the spatial location $X=0.5$. Qualitatively and quantitatively, the curves have relatively little dependence on X, in the first time domain, at least for X between 0.10 and 1.00. It is seen that all Nusselt number curves begin at essentially infinity at time $F=0$ and rapidly decrease with time before a period where they decrease slowly with time. This is due to the zero thickness of the thermal boundary layer at $F=0$ followed by its growth toward $y=R$ as time goes on. The lowest three curves show the dependence of the Nusselt number on the storage ratio B, with Nusselt number Nu increasing as B increases from 0.1 to 10.0. For $B=10.0$, Nusselt number Nu ranges from about 15% higher than Nusselt number Nu for $B=0.10$ to almost 50% higher in the time range $0.10<F<0.35$. Greater and more dramatic changes in the Nusselt number occur as the transient becomes faster at a fixed value of B. This is illustrated by the top four curves in Fig. 6, which are all for $B=10.0$, but for increasing values of g, faster transients, in the expression for generation, $q_g(1+CX)e^{gF}$. Predictions have been made of Nusselt number Nu, using the flux model, for $g=0$, 1, 10, and 20. It is seen that Nusselt number Nu for the higher values of g, at a given time F, are much larger than Nusselt number Nu at smaller values of g. For example, at time $F=0.20$ and 0.35, the value of Nusselt number Nu for $g=20$ is almost 60 and 80%, respectively, higher than its value at $g=0$. By way of comparison, the Nusselt number used in the quasi-steady analysis is shown as the horizontal dashed line. However, as has been pointed out by Sucec,[9] comparison of the actual Nusselt number to the quasi-steady value is not a proper measure of the performance of a quasi-steady analysis, rather, the true assessment of such an analysis is made with comparison of wall temperature and bulk mean temperature as has been done in Figs. 1–5. Finally, some finite difference predictions are also shown in Fig. 6 for $B=0.10$. As has been the case for the other five figures, the model gives results so close to the finite difference results that they coincide to within plotting accuracy. An exception to this is the predicted Nusselt number at $F=0.33$, where the flux model value is 1.7% higher because it is no longer a thermal entrance region at that time.

Conclusions

The two-integral approximate model for the surface heat flux is applied to transient conjugate problems, with wall generation, in the thermal entrance region of a duct during the first time domain, $F\le 2X/3$. The model makes possible an analytical solution to certain of these generation rates. The results of the flux model have been compared to a finite difference solution of the problem without the use of the model. Comparisons have also been made to a simpler quasi-steady approach.

It has been found that the quasi-steady approach can only be used with adequate accuracy for wall temperature if $B\ge 10$ and even the use of $B=10$ still might not give the desired degree of accuracy needed for the bulk mean fluid temperature.

The comparison to finite difference results also indicated that the first time domain solutions can also often be used with acceptable, but decreased accuracy, both to the end of the thermal entrance region or for some time past the end of the first time domain, $F<(\frac{2}{3})X$.

Predicted transient Nusselt numbers depend somewhat strongly on both the thermal energy storage ratio B and on the rapidity of the transient. Faster transients lead to larger values of Nusselt numbers Nu.

Finally, it is hoped that the flux model used here will also be of aid to others in finding analytical solutions to problems involving wall generation rates of interest.

Appendix: Coefficients for Equations (7), (9), (19), and (21–23)

$$C_0 = B\left(-1-\tfrac{5}{4}a_0CB^3+\tfrac{3}{2}a_1CB^4\right)$$

$$C_2 = BC\left(-1-\tfrac{3}{4}a_0B+a_1B^2\right),\qquad C_3 = C\left(2+\tfrac{2}{3}a_0B-a_1B^2\right)$$

$$C_4 = (C/4)(-a_0/2+a_1B),\qquad C_5 = -\tfrac{2}{15}a_1C$$

$$C_7 = CB\left(1-a_0B/2+a_1B^2/2\right)$$

$$A_1 = CB^3\left(a_1B-\tfrac{3}{4}a_0\right),\qquad A_2 = CB(a_1B/2-a_0/4)$$

$$A_3 = CBa_1/3$$

Define $e=g+w$:

$$J_1 = \frac{NuBg[e(1+CX)-C]-CNu^2}{B^2g^2e^2}$$

$$J_2 = \frac{Nu}{B}\left\{\frac{Bw^2e(1+CX)+C[Nu(2g+3w)-Bw(g+2w)]}{Bw^3e^2}\right\}$$

$$J_3 = \frac{Nu}{B}\left\{\frac{C-w(1+CX)}{gw^2}+\frac{NuC}{B}\left[\frac{1}{g^2e^2}-\frac{(2g+3w)}{w^3e^2}\right]\right\}$$

$$J_4 = \frac{NuC(Nu-Bw)}{B^2w^2e},\qquad J_5 = \frac{Nu^2C}{B^2gw^2}$$

$$E_0 = J_3 - \frac{B}{Nu}J_5, \qquad E_1 = J_5, \qquad E_2 = NuJ_1 + 1 + CX$$

$$E_3 = -\frac{(NuJ_2 + J_4)}{NuB}, \qquad E_4 = -\frac{J_4}{B}$$

$$K_0 = \frac{Nu}{Bw^2}\left[-(1 + CX) + \frac{2C}{w} - 3\frac{CNu}{Bw^2}\right]$$

$$K_1 = \frac{Nu}{Bw}\left[(1 + Cx) - \frac{C}{w} + \frac{2NuC}{Bw^2}\right]$$

$$K_2 = -\frac{CNu^2}{2B^2w^2}, \qquad K_3 = -K_0, \qquad K_4 = \frac{CNu}{Bw^2}\left(\frac{Nu}{Bw} - 1\right)$$

$$G_0 = \frac{(1 + CX)}{Nu} + K_0 + \frac{2B^2}{Nu^2}K_2 - \frac{B}{Nu}K_1$$

$$G_1 = K_1 - \frac{2B}{Nu}K_2, \qquad G_2 = K_2$$

$$G_3 = -\frac{1}{B}\left(K_3 + \frac{K_4}{Nu}\right), \qquad G_4 = -\frac{K_4}{B}$$

References

[1]Spiga, M., and Spiga, G., "Transient Temperature Fields in Crossflow Heat Exchangers with Finite Wall Capacitance," *Journal of Heat Transfer*, Vol. 110, No. 1, 1988, pp. 49–53.

[2]Olek, S., "Unsteady Conjugated Heat Transfer in Laminar Pipe Flow," *International Journal of Heat and Mass Transfer*, Vol. 34, No. 6, 1991, pp. 1443–1450.

[3]Al-Nimr, M. A., and Hader, M. A., "Transient Conjugated Heat Transfer in Developing Laminar Pipe Flow," *Journal of Heat Transfer*, Vol. 116, No. 1, 1994, pp. 234–236.

[4]Lin, T. F., and Kuo, J. C., "Transient Conjugated Heat Transfer in Fully Developed Laminar Pipe Flows," *International Journal of Heat and Mass Transfer*, Vol. 31, No. 5, 1988, pp. 1093–1102.

[5]Travelho, J. S., and Santos, W. F. N., "Unsteady Conjugate Heat Transfer in a Circular Duct with Convection from the Ambient and Periodically Varying Inlet Temperature," *Journal of Heat Transfer*, Vol. 120, No. 2, 1998, pp. 506–510.

[6]Sucec, J., and Radley, D., "Unsteady Forced Convection Heat Transfer in a Channel," *International Journal of Heat and Mass Transfer*, Vol. 33, No. 4, 1990, pp. 683–690.

[7]Weng, H. Z., "Unsteady Forced Convection Heat Transfer in the First Time Domain," M.S. Thesis, Mechanical Engineering Dept., Univ. of Maine, Orono, ME, Dec. 1993.

[8]Sucec, J., and Weng, H.-Z., "Transient Conjugate Convection Heat Transfer in a Duct with Wall Generation," *Proceedings of the 33rd National Heat Transfer Conference*, American Society of Mechanical Engineers, Albuquerque, NM, NHTC 99-61 [CD-ROM], 1999.

[9]Sucec, J., "Unsteady Conjugated Forced Convection Heat Transfer in a Duct with Convection from the Ambient," *International Journal of Heat and Mass Transfer*, Vol. 30, No. 9, 1987, pp. 1963–1970.

[10]Sucec, J., "Exact Solution for Unsteady Conjugated Heat Transfer in the Thermal Entrance Region of a Duct," *Journal of Heat Transfer*, Vol. 109, No. 2, 1987, pp. 295–299.

[11]Romie, F. E., "Transient Response of Crossflow Heat Exchangers with Zero Core Thermal Capacitance," *Journal of Heat Transfer*, Vol. 116, No. 3, 1994, pp. 775–777.

[12]Karvinen, R., "Transient Conjugated Heat Transfer to Laminar Flow in a Tube or Channel," *International Journal of Heat and Mass Transfer*, Vol. 31, No. 6, 1988, pp. 1326–1328.